Electromechanical Responses of Strong Acid Polymer Gels in DC Electric Fields

Li Yao† and Sonja Krause*

Department of Chemistry, Rensselaer Polytechnic Institute, Troy, New York 12180

Received August 14, 2002; Revised Manuscript Received January 6, 2003

ABSTRACT: The electromechanical behavior of two cross-linked strong acid hydrogels—(1) 50% sulfonated poly(styrene-*b*-ethylene-*co*-butylene-*b*-styrene) (S-SEBS) and (2) 69% sulfonated polystyrene (S-PS)—were studied in 0.005−0.1 M solutions of Na_2SO_4, Cs_2SO_4, $(CH_3)_4NHSO_4$, and $(C_4H_9)_4NHSO_4$ (TBA) in a 1.6 V/cm dc electric field. Both gels bent toward the cathode when they were preequilibrated in the corresponding salt solutions. The bending angle increased linearly with time at the start and then more slowly toward a steady-state bending angle, θ_{ss}. The time needed to reach θ_{ss} depended on the mobility of the cations, the electric field, and the thickness of each gel, but not on the salt concentration. Both θ_{ss} and the initial speed of bending reached a maximum at the same intermediate salt concentration, C^*, that changed little with type of salt or gel. θ_{ss} decreased while the initial bending speed increased with the mobility of the cation. When the S-PS gel was preequilibrated in distilled water before the bending measurements, the gel first bent toward the anode before reversing toward the cathode in 0.065−0.08 M TBA solutions. The S-PS gel did this in none of the other salt solutions, and the S-SEBS did not reverse its bending behavior at all. The reasons for some of these results are discussed.

Introduction

The electric field-induced deformation of ionic polymer hydrogels has been reviewed recently by Shiga.[1] The phenomena observed depend on a number of factors including the nature of the ionic groups that are part of the hydrogel, whether the hydrogel is allowed to touch the electrodes, the reactions at the electrodes, the nature of the dissolved ions, and the nature of the solvent surrounding the hydrogel. Anionic hydrogels placed in contact with the anode generally shrink when a dc electric field is applied. For example, Tanaka et al.[2] found that a rod-shaped poly(acrylic acid-*co*-acrylamide) gel, when placed between two electrodes in 50/50 acetone/water solution, with the gel touching the electrodes, shrank on the anode side of the gel to 0.005 of its original volume after application of about 0.4 V/cm. Higher electric fields caused shrinkage of the whole gel rod. To explain these phenomena, a competition between the osmotic pressure due to the counterions, the attraction of the positively charged electrode for the negatively charged gel, and the rubber elasticity of the polymer network were invoked. Contractions of hydrogels in the form of rods were later also observed by DeRossi et al.[3] using partially hydrolyzed polyamide and cross-linked poly(sodium acrylate-*co*-vinyl acetate), both when the gel touched the anode and when it was separated from the anode. Using a universal indicator solution, these authors studied the pH gradients set up in the solution and the gel, with the gel separated from both electrodes, after the electric field was turned on. The results indicated that the gels did not start to contract until an acid front, generated at the anode because of the consumption of OH^- there, reached the gel. The changes of pH that were observed in the gel probably resulted in changes in the degree of neutralization of the polymer; this then changed the swelling of the two sides of the gel so that the gel first "curled" and then contracted. Osada et al., who also observed water exudation from some of their gels at the cathode, noted the contraction of gels of poly(2-acrylamido-2-methyl-1-propanesulfonic acid), AMPS,[4] cross-linked poly(methacrylic acid), PMAA,[5] and microparticles of cross-linked poly(acrylic acid), PAA,[6] after they migrated to the anode. Most of the hydrogels mentioned above contained weak acid groups so that the concentrations of these groups in the gels could change not only because of changes in the swelling of the gels but also because of changes in the degree of neutralization of the acid groups.

Slabs of ionic hydrogels that are attached at one end or in the middle so that they cannot contact either electrode generally bend toward one of the electrodes in a dc electric field. Negatively charged hydrogels usually bend toward the cathode, but not in all cases. For example, according to Shiga and Kurauchi,[7] some gels of partly neutralized poly(acrylic acid-*co*-acrylamide) that had been equilibrated in distilled water and were then placed in NaOH solution in an electric field without contacting either electrode had ends that bent toward the cathode only at NaOH concentrations below 10^{-3} M; at higher NaOH concentrations they bent toward the anode. However, gels with smaller degrees of neutralization bent first toward the anode and only later toward the cathode. Optical density measurements at 225 nm showed that the concentration of $-COO^-$ groups in the gels decreased markedly when the gel bending reversed. Many of these observations were explained using calculations of the osmotic pressure differences between the anode and cathode sides of the gels as a function of time using the changes of Donnan equilibrium[8] with time that developed as a result of mobile ion transport through the solution and the gel. The amount of swelling of different portions of the gel depends not only on the osmotic pressure within each portion of the gel but also on the amount of cross-linking. The observed degree of gel bending was used to calculate a value of Young's modulus for the swollen

† Present address: Department of Chemical Engineering, Virginia Commonwealth University, Richmond, VA.

10.1021/ma021326q CCC: $25.00
Published on Web 02/22/2003

gel, assuming that the bending resembled a three-point bending test. Calculated and experimental values of Young's modulus were compared, but the method for obtaining comparable experimental values was not explained. We may note that Shiga and Kurauchi's gels were not preequilibrated in the solutions in which their behavior in an electric field was observed.

Polymer gels with strong acid groups, which completely dissociate in salt solutions except at very low pH, were studied, among others, by Kwon et al.,[9] Choi et al.,[10] and Ye et al.[11] In a study of cross-linked poly(2-acrylamido-2-methylpropanesulfonic acid-*co*-butyl methacrylate) (PAMPS-*co*-BMA) rectangular gels without electrode contact, Kwon et al.[9] noted that all their gels bent reversibly toward the cathode in electric fields. The bending angles and times to reach a stable bending angle increased with an increase of the applied voltage. The maximum bending angle increased linearly as the cross-link density of the gel decreased, that is, when the swelling ratio of the gel increased. These authors also studied the pH changes that occurred inside an electrically stimulated gel in distilled water and the amount of water that moved through the gel under the same conditions; their other measurements, however, were done in salt solution. Since they could not relate the amount of differential swelling on the anode and cathode sides of their membranes needed to explain their bending data either to their measured pH changes or water transport, and since they were able to measure large changes in swelling ratio of their membranes in NaCl solutions of different ionic strength, Kwon et al.[9] inferred that the bending angle was solely due to the ionic strength dependence of the swelling ratios of the anode and cathode sides of the gel.

Choi et al.[10] studied the reversible bending in an electric field of both a neutral polyacrylamide gel and an anionic AMPS gel. The direction of bending of the neutral gel after application of the electric field, whether toward the anode or toward the cathode, depended on the binding of mobile ions on the gel. The AMPS gel bent reversibly toward the cathode and the bending angle decreased after reaching a maximum. Choi et al.[10] attributed the final decrease of bending angle to the very low pH, ~1.5, that developed at the anode because of water electrolysis while the electric field was on; this resulted in the protonation of the strong acid sulfonate groups on the anode side of the gel, thus decreasing its swelling with respect to the cathode side of the gel.

A linear, partially sulfonated poly(styrene-*b*-ethylene/butylenes-*b*-styrene) (S-SEBS) gel in 0−0.2 M Na_2SO_4 solutions was studied by Ye et al.[11] Each gel was swollen in the appropriate salt solution for more than 24 h before the electric field was applied. The bending angle had a maximum value in 0.02 M Na_2SO_4 and was larger in all solutions at higher sulfonation of the gel. Also, the bending angle increased as the electric field increased, but with some leveling off at higher fields. Unfortunately, this gel was not chemically cross-linked, so that swelling equilibrium was never reached. In distilled water, the gel dissolved after about 273 days; a gel in 0.02 M Na_2SO_4 solution was monitored up to the 273rd day and was still swelling slowly at that time.[12]

The most comprehensive theoretical interpretation of hydrogel bending data at this time is that of Doi et al.,[13] who proposed a quantitative theory for the swelling behavior of weak acid gels at different pH's in salt solution in an electric field. They considered the diffusion and electrical mobility of the ions in the electric field in addition to the Donnan equilibrium at all times at each gel boundary. In a quantitative numerical calculation using a 1:1 electrolyte, they calculated the time dependence of the osmotic pressure at the gel boundaries since this controls the different swelling of the gel at the anode and cathode sides of the gel and thus the bending of the gel. In this quantitative calculation, the same diffusion constant, and thus the same electrical mobility, was used for all mobile ions in order to simplify the calculations. However, in reality, the different ions have different diffusion coefficients. Because of this, one purpose of the present work was to study the effect of different cations with different diffusion coefficients, and thus different mobilities, on the gel bending. The bending behavior of two strong acid gels, partially sulfonated cross-linked polystyrene, S-PS, and cross-linked S-SEBS, were studied in four different electrolytes over a range of concentrations in dc electric fields without electrode contact.

Experimental Section

Cross-Linked S-SEBS Gel. Fifty percent sulfonated S-SEBS, as determined by titration, was obtained from the DIAS Corp. (now DIAS Analytical Corp., Odessa, FL) in 1-propanol/cyclohexane solution. The original nonsulfonated block copolymer contained 29 wt % styrene. Thin films of S-SEBS, about 0.25−0.3 mm thick, were obtained by casting from solution into Petri dishes; these films were neutralized in NaOH solution and washed in distilled water until the wash water was neutral. After drying under vacuum at room temperature, the films were chemically cross-linked using Co-60 γ-ray irradiation at the Ward Center for Nuclear Science, Cornell University, Ithaca, NY. S-SEBS films dosed with 10, 15, and 20 Mrad were prepared and named S-SEBS-10, S-SEBS-15, and S-SEBS-20. These cross-linked S-SEBS gels were used for further studies only after the soluble polymer had been extracted using a Soxhlet extractor at 70 °C using tetrahydrofuran as solvent.

Partially Sulfonated Cross-Linked Polystyrene Gel: Synthesis. Lightly cross-linked polystyrene networks were synthesized by bulk free radical polymerization of styrene monomer with divinylbenzene (DVB), both from Aldrich Chemical Co., Milwaukee, WI. Prior to polymerization, both the styrene and the DVB were washed with 10% NaOH solution three times to remove the inhibitor (4-*tert*-butylcatechol), then rinsed with distilled water until the pH of the rinsed water was neutral, and dried with molecular sieves. Benzoyl peroxide, BPO, Aldrich Chemical Co., was dissolved in a DVB/styrene mixture with mole ratio 0.005. A gasket consisting of a piece of vinyl tubing was used to separate two glass plates, and the plates were clamped together. The monomer/initiator mixture was then transferred to the volume between the glass plates under N_2 and allowed to react at 70 °C for 12 h in a water bath. Typically, a 1 mm thick polymer slab was obtained.

Sulfonation. The sulfonating reagent, acetic sulfate, was prepared following the procedure described by Makowski et al.[14] A 90 mL aliquot of acetic anhydride was added to 300 mL of dichloroethane in an ice bath. After the solution had cooled to <10 °C, 30 mL of 95% sulfuric acid was slowly added. A 5 g slab of cross-linked polystyrene was allowed to swell in 300 mL of dichloroethane for 3 h, and then the swollen slab was transferred to the sulfonating reagent mixture and allowed to swell overnight in the ice bath. Then the mixture was heated to 50 °C and stirred constantly for 5 h, and the reaction was terminated by addition of 100 mL of 1-propanol. The polymer slab was then soaked in a mixture of 100 mL of 1-propanol and 50 mL of ethanol overnight, washed repeatedly with ethanol, and dried in a vacuum oven at room temperature

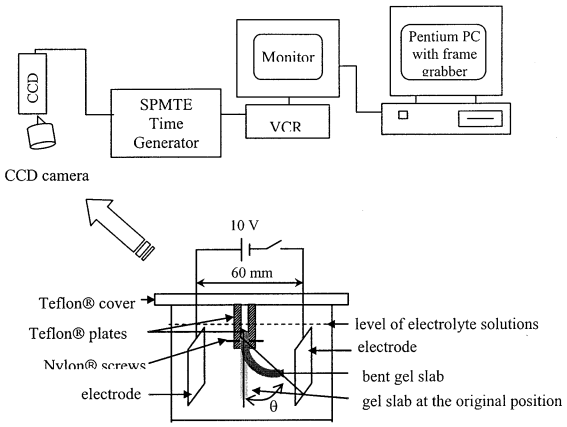

Figure 1. A schematic of the instrumentation used to study gel bending. The angle θ is the bending angle as defined in the text.

for 2 days. The sample used for the studies discussed in this paper contained 12.65 wt % S as determined by Atlantic Microlab Inc., Norcross, GA, using sulfur elemental analysis (duplicate measurements). This sulfur content is equivalent to a sulfonated styrene content of 69.3 mol % (81.7 wt %).

Swelling Measurements. The neutralized S-SEBS gels were dried in a vacuum oven at room temperature to constant weight and then cut into 1 × 1 cm squares while the neutralized S-PS gels were dried to constant weight in air but otherwise treated the same way. After immersion in the swelling solution, the swollen gel samples were blotted to remove solution on the surfaces, weighed, and placed back into the same solution. This procedure was repeated until constant weight was reached. The ratio of the weight of the swollen gel at equilibrium to the weight of the dry gel was the equilibrium swelling ratio.

Electromechanical Responses. The electromechanical response of the gels was studied in the cell shown in Figure 1. All gel slabs, except when specified, were allowed to swell to equilibrium in the solution to be used for the bending studies before use. The wet S-SEBS slabs were approximately 1 × 0.5 × 0.025 cm (length × width × thickness) while the wet S-PS slabs were 1 × 0.5 × 0.15 cm, where the length is the distance from the point where the gel was clamped to its dangling free end in solution. A piece of swollen gel slab was placed halfway between two stainless steel plate electrodes, 2.5 × 2.5 cm, 6 cm apart, with one end of the gel slab fixed by clamping it between two Teflon plates using two sets of nylon screws. The gel slab and the electrodes faces were parallel to each other and immersed in electrolyte solutions. Ten volts dc (Lambda model LK342A FM regulated dc power supply, Lambda Electronic Corp., Melville, NY) was used in all electromechanical response experiments. The bending response of each gel was recorded using a black and white Hamamatsu XC-77 CCD camera (Hamamatsu Corp., Japan) that was connected to a SMPTE time code generator/reader (model TC-3, Burst Electronics Inc., Corrales, NM), then to a VCR, a SONY monitor, and finally to a PC which had an Imaging Technology CFG (VP-1300-640) interface. The bending angle, θ, defined as the angle between the initial vertical position of the gel and the straight line drawn between the attached upper end of the gel slab and its lower tip in the final steady state position as shown in Figure 1, was measured using the Optimas Imaging Analysis software, version 6.1 (Optimas Corp., Bothell, WA). Even though this method of characterizing the degree of bending is somewhat arbitrary and varies with the length and thickness of the gel, it has been used previously by many workers.[7,9−12,15] The electromechanical responses of the gels in sodium sulfate, cesium sulfate, tetramethylammonium hydrogen sulfate (TMA), and tetrabutylammonium hydrogen sulfate (TBA) at concentrations between 0.005 and 0.1 mol/L were studied. All salts were from the Aldrich Chemical Co., Milwaukee, WI.

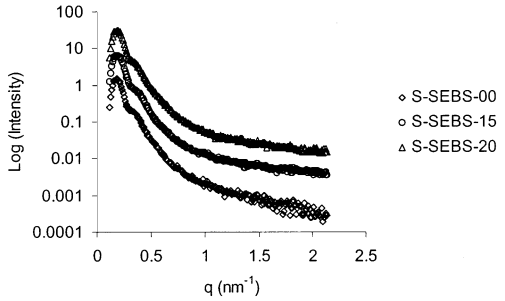

Figure 2. SAXS curves of dry S-SEBS: (◊) un-cross-linked S-SEBS, (○) cross-linked S-SEBS-15, (△) cross-linked S-SEBS-20. For clarity, the curves of S-SEBS-15 and S-SEBS-20 have been shifted vertically upward by multiplying their original intensities by 5 and 20, respectively.

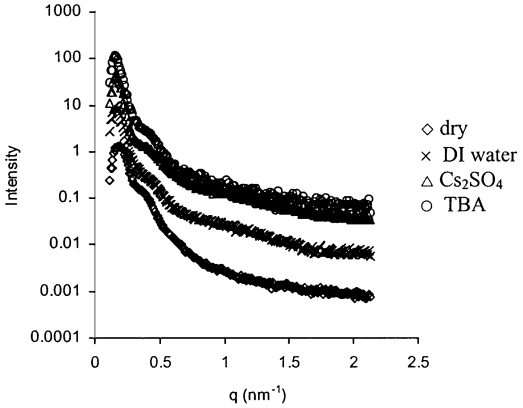

Figure 3. SAXS curves of dry and swollen samples of S-SEBS-15: (◊) dry film, (×) in deionized water, (△) in 0.03 M Cs_2SO_4, (○) in 0.03 M TBA. For clarity, the curves of the films swollen in deionized water, 0.03 M Cs_2SO_4, and 0.03 M TBA solutions were shifted upward vertically by multiplying the original intensities by 10, 40, and 250, respectively.

Small-Angle X-ray Scattering (SAXS). The SAXS experiments of S-SEBS films were carried out at the Department of Polymer Science and Engineering, University of Massachusetts, Amherst, at room temperature using filtered 1.54 Å Cu Kα radiation and a 2D detector. A piece of S-SEBS film was stuck onto a piece of Kapton film. The sample-to-detector distance was 1 m, covering a scattering vector (q) range from 0.01 to 0.21 Å^{-1}, where $q = (4\pi/\lambda)\sin(\theta/2)$; θ is the scattering angle and λ is the wavelength of the X-ray. Both dry and swollen samples of S-SEBS were studied.

Results and Discussion

Morphology of S-SEBS. The S-SEBS is a triblock copolymer whose morphology can change with percent sulfonation, percent neutralization, and amount of swelling. SAXS data were used to obtain some information on the morphology of the cross-linked polymers, both dry and swollen. The SAXS profiles of un-cross-linked and cross-linked S-SEBS samples in the dry state are shown in Figure 2, while Figure 3 shows the SAXS profiles of swollen cross-linked S-SEBS-15 in different salt solutions. The SAXS curves of un-cross-linked dry S-SEBS and both cross-linked dry S-SEBS samples are almost the same. Therefore, as might be expected, the morphology of the S-SEBS was not affected by cross-linking. To estimate this morphology, we took the ratio of the q value of the second, not well-resolved observed scattering peak, q_2, to that of the first, q_1; one or two additional orders of diffraction would be necessary for a better estimate. At any rate, for a face-centered-cubic lattice of spheres, this ratio is 1.15, for a simple or body-

Table 1. q Values of the First and Second SAXS Scattering Peaks of the S-SEBS Samples[a]

	un-cross-linked S-SEBS			S-SEBS-15			S-SEBS-20		
solvent	q_1 (nm^{-1})	q_2 (nm^{-1})	q_2/q_1	q_1 (nm^{-1})	q_2 (nm^{-1})	q_2/q_1	q_1 (nm^{-1})	q_2 (nm^{-1})	q_2/q_1
none	0.185	0.321	1.73	0.185	0.321	1.73	0.185	0.322	1.74
H_2O[b]	0.149	0.365	2.45	0.158	0.393	2.49	0.161	0.394	2.45
Na_2SO_4	0.156	0.384	2.46	*c*	*c*	*c*	*c*	*c*	*c*
Cs_2SO_4	0.156	0.407	2.61	0.168	0.417	2.48	0.171	0.421	2.46
TBA	*c*	*c*	*c*	0.163	0.424	2.60	0.165	0.391	2.37

[a] All salt solutions had a concentration of 0.03 M. [b] Deionized. [c] Data not obtained.

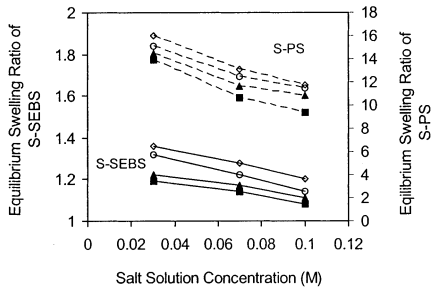

Figure 4. Equilibrium swelling ratios of the S-SEBS (solid lines) and S-PS (dashed lines) gels in Cs_2SO_4 (◇), Na_2SO_4(○), TMA (▲), and TBA (■).

centered-cubic lattice of spheres it is 1.42, for a hexagonal arrangement of infinite cylinders the ratio it is 1.73, and for a regular lamellar morphology the ratio it is 2.0.[16] Table 1 summarizes the values of this ratio of all the samples investigated. The value of all the dry S-SEBS samples was ∼1.73, the characteristic value for the cylindrical morphology. This indicates that all the dry S-SEBS gels, regardless of the degree of cross-linking, were probably microphase separated into a cylindrical morphology. Cylindrical morphology has been obtained for similar triblock copolymers containing styrene end blocks and a hydrocarbon center block, for example, in the case of a styrene−butadiene-styrene triblock copolymer containing 30 wt % styrene.[17] In the swollen S-SEBS samples, both un-cross-linked and cross-linked, the first scattering peak shifted toward to lower q values, while the second scattering peak moved to higher q values. The shift of q_1 to lower values was consistent with the swelling of the gels; this should increase the distance between the microphases in the gels.

Assuming that q_1 is a first-order Bragg peak, the average domain spacing between neighboring microphases, L, can be determined from Bragg's law

$$L = \frac{2\pi}{q_1} \tag{1}$$

and are as follows: dry S-SEBS-15, ∼34 nm; S-SEBS-15 swollen with deionized water, ∼40 nm; 0.03 M Cs_2SO_4 or 0.03 M TBA, ∼38 nm. The swollen S-SEBS-15 samples had q_2/q_1 values between 2.4 and 2.6, not characteristic of either a cylindrical or any other simple morphology. This is understandable since almost all of the swelling must be in the sulfonated polystyrene cylinders, and this swelling would almost certainly result in a changeover into another morphology if it were not hindered by the chemical cross-links.

Equilibrium Swelling. The experimentally determined equilibrium swelling ratios of the gels as a function of salt and salt concentrations are shown in Figure 4. The equilibrium swelling of the S-PS gel was greater than that of the S-SEBS gels under similar conditions. This is reasonable since the S-SEBS gels contain a large proportion of hydrocarbon block that does not take part in the swelling. The degree of equilibrium swelling of both types of gel decreased with increasing external salt solution concentration and was higher in 1−1 salts than in 1−2 salts at the same salt concentration. These data can be explained qualitatively through a discussion of the osmotic pressure differences across the boundaries of the polymer gel with the surrounding salt solution even though the swelling behavior of ionic polymer gels is partly governed by two other factors. These are (1) the ionic interactions between the fixed charges on the polymer backbone and the mobile ions in the salt solution and (2) the elasticity of the polymer network.

When an ionic polymer gel swells in a salt solution, the swelling equilibrium and the distribution of the ions in the gel and the surrounding solution are usually described by the Donnan equilibrium. This equilibrium involves electroneutrality both inside the gel and in the surrounding solution and equal chemical potential of the salt inside and outside the gel. For a monovalent anionic gel swelling in 1−1 salt, the Donnan equilibrium conditions, assuming the same mean ionic activity coefficient of the salt inside and outside the gel, are

$$C_g^- = C_s\sqrt{1 + \frac{1}{4}\left(\frac{zC_{g,P}}{C_s}\right)^2} - \frac{zC_{g,P}}{2} \tag{2a}$$

$$C_g^+ = C_s\sqrt{1 + \frac{1}{4}\left(\frac{zC_{g,P}}{C_s}\right)^2} + \frac{zC_{g,P}}{2} \tag{2b}$$

where C_s is the molar concentration of the salt in the solution outside the gel, C_g^- and C_g^+ are the molar concentrations of the negative and positive ions of the salt in the gel, respectively, $C_{g,P}$ is the molar concentration of fixed ions in the gel, and z is the charge of each fixed ion. In the case of the 2−1 electrolytes, C_g^- and C_g^+ can be obtained, using the same assumptions as for 1−1 electrolytes, by solving the following third degree equations:

$$(C_g^+)^3 - zC_{g,P}(C_g^+)^2 - 8C_s^3 = 0 \tag{3a}$$

$$4(C_g^-)^3 + 4zC_{g,P}(C_g^-)^2 + z^2(C_{g,P})^2C_g^- - 8C_s^3 = 0 \tag{3b}$$

At relatively low salt concentrations, otherwise using the same assumptions used for eqs 2a,b and 3a,b, the osmotic pressure difference, Π, between the gel and the outside solution can be written

$$\Pi = RT\sum_i (C_{i,g} - C_{i,s}) \tag{4}$$

where R is the universal gas constant, T is the absolute temperature, and $C_{i,s}$ and $C_{i,g}$ are the concentrations of

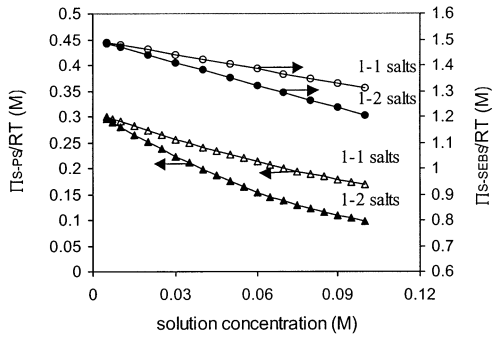

Figure 5. Estimated osmotic pressure differences between the gels and the external salt solutions.

ions of type I in the solution and in the gel, respectively. At swelling equilibrium, $C_{i,s}$ and $C_{i,g}$ are calculated from the Donnan equilibrium condition, in our two cases either eqs 2a,b or eqs 3a,b.

To use eqs 2a,b and 3a,b, $C_{g,P}$ in the two gels must be estimated. In the case of the S-PS gel, the molar concentration of sulfonated groups in the dry gel was calculated first and then corrected for the degree of swelling of the gel. To do this using the 81.7 wt % sulfonated styrene units found experimentally in the gel, it was necessary to estimate its dry density. This was done by using 1.05 and 0.81 g/cm^3 for the densities of polystyrene and sodium polystyrenesulfonate, respectively, and assuming that these repeat units contributed the densities of the homopolymers to the copolymer. This gave the density of the dry copolymer as 0.88 g/cm^3. $(C_{g,P})_{S-PS}$, the molar concentration of charges in the swollen gel, could then be estimated at the different swelling ratios using the equilibrium swelling ratio of the gel, Q_m, in the solution of interest, assuming zero volume change on mixing. Using these values and assumptions, $(C_{g,P})_{S-PS}$ was, in moles per liter,

$$(C_{g,P})_{S-PS} = \frac{3.95}{Q_m + 0.14} \tag{5}$$

In the case of the S-SEBS gel, an additional assumption was necessary. We assumed that only the sulfonated styrene microphases were swollen in the solutions and that the EB microphases remained dry. In this case, $(C_{g,P})_{S-SEBS}$, the molar concentration of charges in the partially sulfonated polystyrene portion of the swollen gel was

$$(C_{g,P})_{S-SEBS} = \frac{1.39}{Q_m - 0.66} \tag{6}$$

Figure 5 shows the estimated Π of both gels using eqs 4−6 for both 1−1 and 1−2 salts. Considering all the assumptions made in the calculations underlying the curves in Figure 5, these curves are at least qualitatively similar to the equilibrium swelling data in Figure 4. The major difference involves the dependence of the experimental curves of Figure 4 on the chemical nature of the counterions while no such dependence, for neither 1−1 nor 1−2 salts, was observed in the calculations of the osmotic pressure difference between the gels and the solutions. Both gels swelled more in Cs^+ salt than in Na^+ salt and more in TMA than in TBA. A similar dependence of the swelling on the chemical nature of the counterions was observed by Liu et al.[18] in cross-linked poly(2-acrylamido-2-methylpropanesulfonic acid) (PAMPS) gels in which the equilibrium swelling ratio

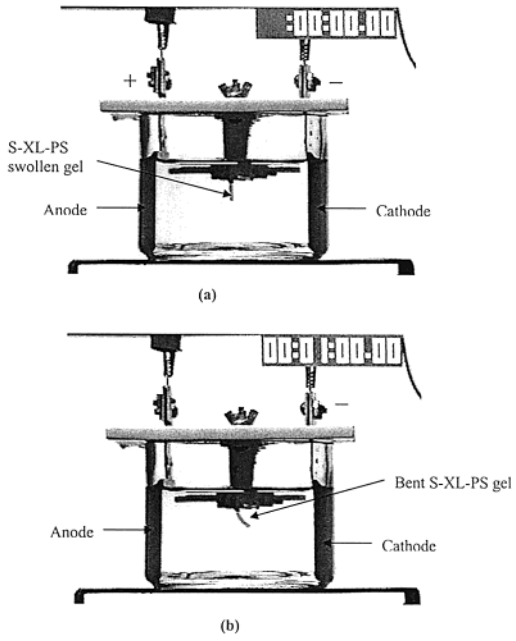

Figure 6. Photographs of the of the S-PS in 0.03 M Na_2SO_4 solution (a) before the electric field was turned on and (b) 1 min after a 1.6 V/cm electric field was applied.

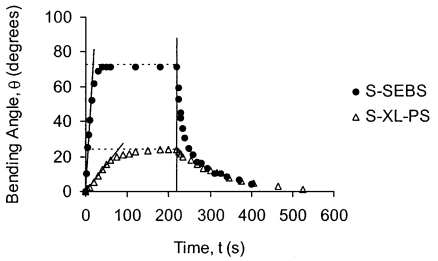

Figure 7. Bending angles of both gels as a function of time. The vertical straight line at $t = 210$ s indicates the time when the electric field was turned off. The area to the left of this line represents the time that the electric field was on; to the right of the line, the electric field was off.

decreased from K^+ salts to Na^+ salts to Ca^{2+} salts at the same ionic strength with essentially no effect of the anions, Cl^- or SO_4^{2-}. They felt this counterion dependence of the swelling was connected with counterion condensation on the charged gels.

Electromechanical Response as a Function of Time. When a 10 V electric field, equivalent to 1.6 V/cm dc, was applied to the gel slabs which had been pre-equilibrated in the same salt solution as was used in the experiment, both S-SEBS and S-XL-PS gels bent toward the cathode as shown for the S-PS gel in 0.03 M Na_2SO_4 in Figure 6. This is consistent with the work on anionic polymer gels[7,9−11,15] discussed earlier in this paper. Figure 7 shows typical gel bending curves of both the S-SEBS and S-PS gels as a function of time. Both gels began to bend immediately after the electric field was turned on. The gel bending angle, θ, increased rapidly and linearly at the beginning and then leveled off to a steady-state bending angle, θ_{ss}. When the electric field was shut off, the gels gradually relaxed to their original straight perpendicular position. This bending behavior could be repeated many times. Because of the shapes of the bending curves when the electric field was on, we tried to use inverse exponentials to describe the bending process. However, the increase of the bending angle did not generally fit an inverse exponential

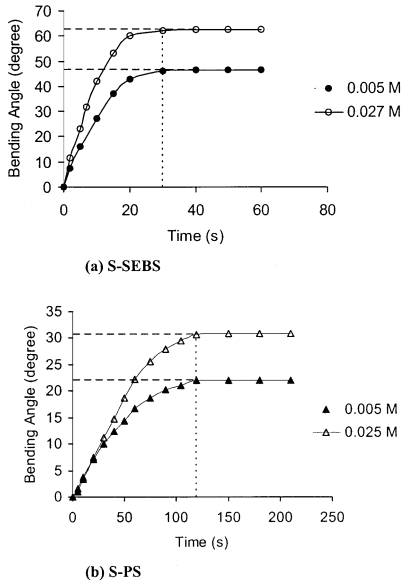

Figure 8. Bending angles vs time and t_{ss} of (a) S-SEBS and (b) S-PS in Cs_2SO_4 solutions at different concentrations.

Table 2. Approximate Hydrated Radius (*r*), Ionic Mobility (μ), Diffusion Coefficient (*D*), and Drift Velocity (*s*) of the Ions in Dilute Aqueous Solution at 25 °C

ion	*r* (nm)	$\mu \times 10^4$ ($cm^2\ s^{-1}\ V^{-1}$)[c]	$D \times 10^5$ ($cm^2\ s^{-1}$)[b]	$s \times 10^4$ (cm/s)[d]
Cs^+	0.25[a]	7.99	2.056	12.8
Na^+	0.4[a]	5.19	1.334	8.3
$(CH_3)_4N^+$	0.45[a]	4.65	1.196	7.4
$(C_4H_9)_4N^+$		2.02	0.519	3.23
SO_4^{2-}	0.4[a]	8.29	1.065	13.3
HSO_4^-	0.4[a]	5.10	1.311	8.16

[a] From Lange's *Handbook of Chemistry*.[20] [b] From the *Handbook of Chemistry and Physics*.[21] [c] Calculated from the diffusion coefficient using equation. [d] Calculated using eq 8 and the applied electric field of 1.6 V/cm.

function. Instead, the bending angle increased linearly (linear regression coefficients were between 0.96 and 0.999) at the beginning of the bending curve in all cases. From this linear portion of each bending curve, the initial speed of bending, $V_{ini} = d\theta/dt$, was obtained. The time needed to reach the steady-state bending angle, t_{ss}, had to be estimated. This could be done in a rough way by drawing a horizontal straight line through the steady-state bending angle data and the time at which this straight line met the rise portion of the curve was estimated as shown in Figure 8. This procedure is so arbitrary that the true t_{ss} was estimated from the numerical values of the bending angle obtained from the image analysis software at different times. These values were calculated at 5, 10, or 20 s intervals, depending on the gel, and t_{ss} was assumed to be in the interval just before the bending angle reached a constant value.

Neither the S-SEBS nor the S-PS gel responded to the electric field in deionized water but bent in salt solutions. This implies that the salt solutions are indispensable for the gel bending. Table 2 shows some relevant properties of the ions in these salt solutions. Figures 9−12 compare the steady-state bending angle and initial speed of bending of the two gels as a function of concentration in all the salt solutions. Note that the S-SEBS gel bent past the 90° mark at some concentrations in TBA solution (Figure 12). This may be caused by a buoyant effect from the combination of the large

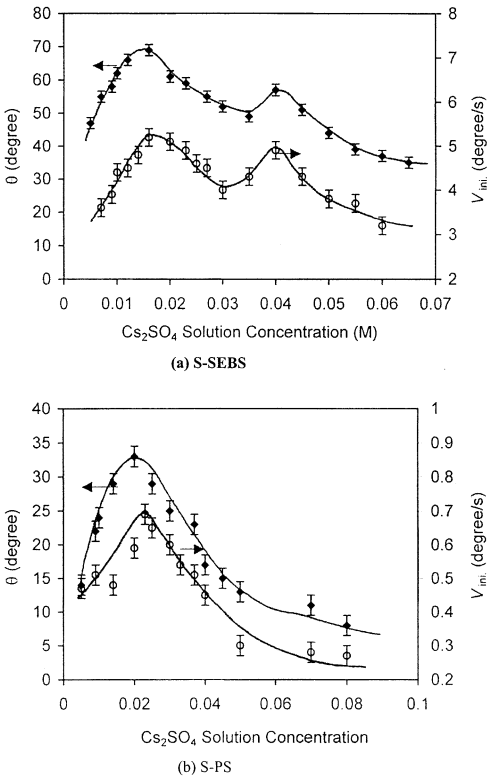

Figure 9. Effect of salt concentration on the steady-state bending angle and initial speed of bending of (a) S-SEBS and (b) S-PS gels in Cs_2SO_4.

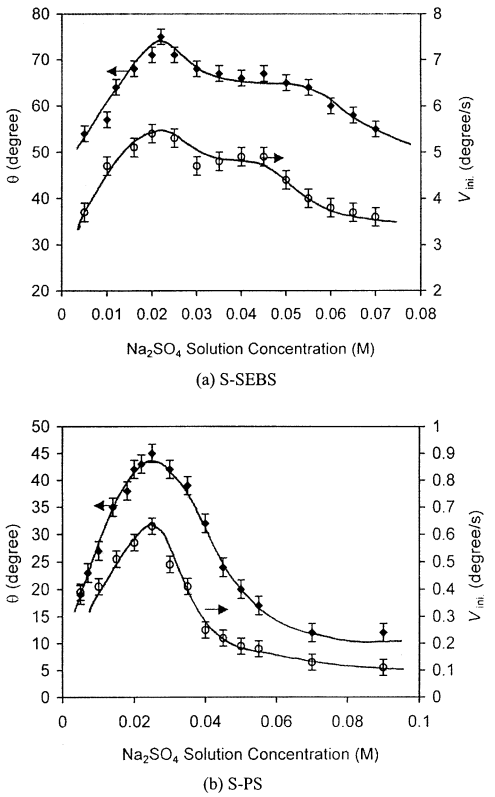

Figure 10. Effect of salt concentration on the steady-state bending angle and initial speed of bending of (a) S-SEBS and (b) S-PS gels in Na_2SO_4.

swelling of the gel and the large bending angle (somewhat less than 90° without the buoyant effect). For both gels, the steady-state bending angle and initial speed of bending at first increased with increasing salt con-

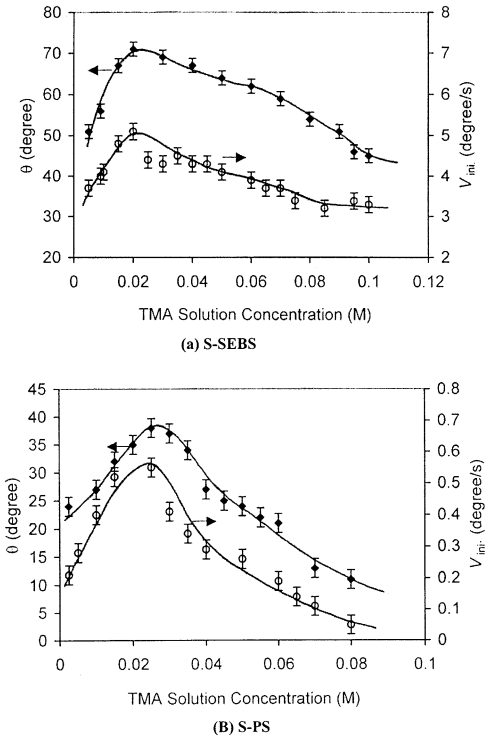

Figure 11. Effect of salt concentration on the steady-state bending angle and initial speed of bending of (a) S-SEBS and (b) S-PS gels in TMA.

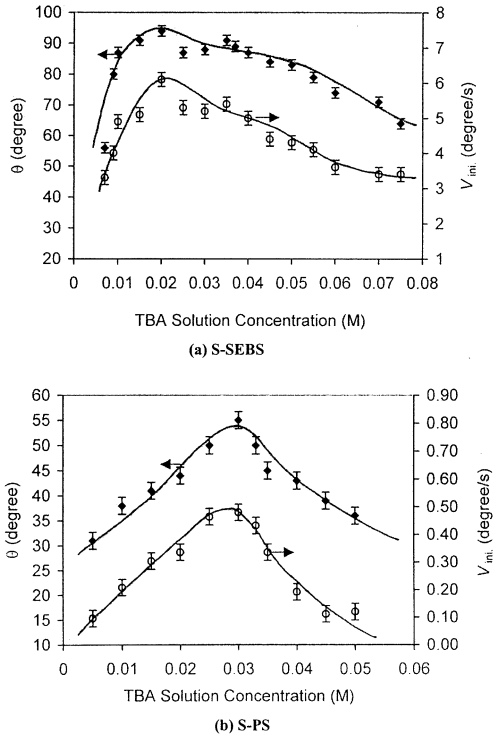

Figure 12. Effect of salt concentration on the steady-state bending angle and initial speed of bending of (a) S-SEBS and (b) S-PS gels in TBA.

centration, reaching a maximum and then decreasing again. In the case of the S-PS gel, both the steady-state bending angle and initial speed of bending decreased consistently as the salt concentration increased further, except for a slight plateau in TMA solution. However, in the case of the S-SEBS gel, secondary peaks were observed at a higher salt concentration in all the salts except TMA. Even in TMA solution, however, there is evidence for a broad plateau that might conceal a second peak. In earlier work, Ye[11,12] reported a maximum steady-state bending angle for an un-cross-linked, also ∼50% sulfonated S-SEBS sample in ∼0.02 M Na_2SO_4 (data obtained from 0.001 to 0.2 M). Our cross-linked S-SEBS sample was studied in a more limited concentration range (0.005−0.07 M), but the two curves are within experimental error of each other, with the same maximum steady-state bending angle. This is hard to see, because Ye[11,12] used a logarithmic concentration axis. Nevertheless, it looks as if cross-linking did not change the bending angle of S-SEBS in Na_2SO_4.

Comparing the bending curves of S-SEBS with those of S-PS in the various salt solutions (Figures 9−12), the curves of S-SEBS are all broader than those of S-PS. This implies that the bending of S-SEBS must be affected by an additional factor beyond the bending of S-PS. This factor is probably connected with the morphology, and possible changes of morphology with salt concentration, of the S-SEBS block copolymer in solution. Our SAXS data, discussed above, has shown that there is a change in morphology during swelling of this block copolymer, at least in the cross-linked samples. Ye's published data on un-cross-linked, 10-day swollen samples indicate that these samples probably had the same morphology changes during swelling.

Figures 9−12 show that the influence of salt concentration on the steady-state bending angle and the initial speed of bending are almost the same. This parallel relationship implies that the degree of steady-state bending and initial speed of bending are controlled by the same variables.

Some of these variables were noted by Homma et al.,[15] who studied the initial speed of bending of a membrane prepared using an interpenetrating network (IPN) of poly(vinyl alcohol) and poly(2-acrylamido-2-methylpropanesulfonic acid, PVA−PAMPS, in Na_2SO_4 and in $CuSO_4$ solution. It is not entirely clear from their paper whether they used exactly the same definition for the bending angle as we did, but they did use the position of the tip of the hanging membrane to calculate this angle in a manner close to the one used in the present paper. At any rate, they also reported an initial linear bending rate and a maximum bending rate at an intermediate salt concentration in solutions of both salts that increased as the concentration of fixed charges on the gel increased. When they plotted initial bending rate vs the inverse of the initial Donnan ratio, K, where

$$K = \left(\frac{C_{i,g}}{C_{i,s}}\right)^{1/z_i} \tag{7}$$

with $C_{i,g}$ and $C_{i,s}$ as the concentration of one of the mobile ions in the gel and the outside solution, respectively, and z_i the charge on this ion, the curves for the different gels with different concentrations of fixed charges could be superimposed for each salt separately. The values of K at which the initial bending rate had its maximum was almost the same for the two salts. These workers used essentially the same equations, with the same underlying assumptions, as eqs 2a,b and 3a,b in the present paper, to calculate $C_{i,g}$. The values of $C_{g,P}$ used in their calculations were stated to be that "at the preparation stage of the membrane", probably before swelling. Maximum bending speed occurred at the same deswelling ratio of each gel membrane; this

Table 3. Maximum Steady-State Bending Angle (θ*), the Maximum Initial Speed of Bending (V_{ini}*), and the Salt Concentration (C*) at Which These Maxima Occurred

	S-SEBS			S-PS		
salt	C* (M)	θ* (deg)	V_{ini}* (deg s^{-1})	C* (M)	θ* (deg)	V_{ini}* (deg s^{-1})
Cs_2SO_4	0.016	69	5.2	0.02	33	0.69
Na_2SO_4	0.02	71	5.4	0.025	45	0.63
TMA	0.02	71	5.1	0.025	38	0.55
TBA	0.02	94	5.1	0.03	55	0.48

was defined as the ratio of the volume of the gel at a certain salt concentration divided by its maximum volume, presumably in distilled water. The authors concluded that the fastest bending speeds occurred when (a) there was a large initial concentration difference in mobile ion concentration across the gel boundaries (large Donnan ratio), (b) a very different change in the Donnan ratio across the gel boundary on the anode side of the gel versus that on the cathode side of the gel as ions begin moving from one electrode to the other went through the gel (this will be clarified below), and (c) high conductivity of the electrolyte solution to induce quick changes in ionic concentration across the gel boundaries. Homma et al.[15] also found that the initial bending speed of their gels varied with the inverse 1.7 power of the gel thickness for each type of gel (type of gel refers to a particular fixed ion concentration) in a particular electrolyte with a particular concentration. The thinner the piece of gel, the faster it bent.

The work discussed in the present paper involves two different types of gel, not the same type of gel with different concentrations of fixed ions. Thus, additional information could be obtained. Table 3 summarizes the maximum steady-state bending angle (θ_{ss}*), the maximum initial speed of bending (V_{ini}*), and the salt concentration (C*) at which these maxima occurred for both gels. For both gels, the C*'s are almost the same in all the salts, averaging 0.022 M. However, both the steady-state bending angle and initial speed of bending were very different for the two gels, and in the case of each gel separately, they varied with salt, especially in the case of the S-PS. Thus, some properties of the salts must be important for an understanding of the bending phenomena. The most likely properties are the size and mobility of the hydrated cations since these are the dominant mobile ions in our gels. Since the hydrated radii of the cations vary inversely with their mobility (see Table 2), either variable could be used for discussion. We shall use the mobility since this variable is intimately involved with our experiments, and values were available for all our mobile ions.

Figure 13 shows how the maximum initial speed of bending and the maximum steady-state bending angle varied with the mobility of the hydrated cations. Thus, at the approximately constant concentration at which these maximum values occurred, the steady-state bending angle decreased almost linearly while the initial speed of bending increased almost linearly as the mobility of the hydrated cation increased. The bulkier the hydrated cation, the less its mobility, causing a slower maximum bending speed but a larger maximum steady-state bending angle. This correlation, to be discussed with some other correlations later, existed at all the salt concentrations studied in this work.

A rather different system, studied by Oguro et al.,[19] also showed a dependence of bending angle on the size of the hydrated cations in the gel. But this system

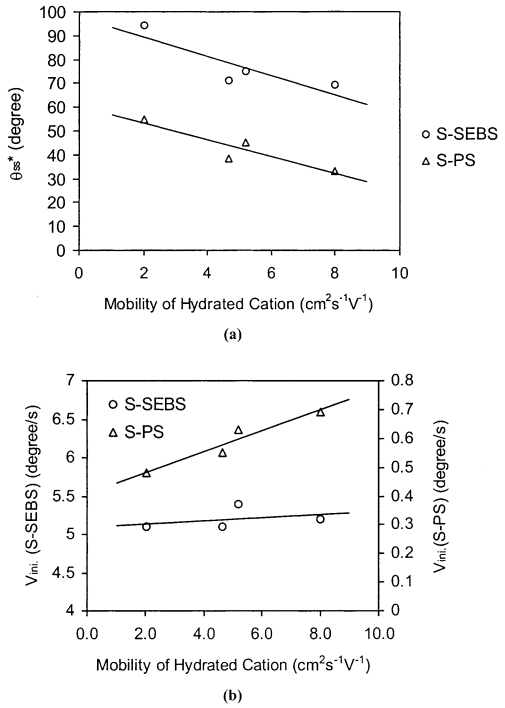

Figure 13. Maximum steady-state bending angle (a) and initial bending speed (b) vs the mobility of the hydrated cations.

consisted a gold-plated Flemion (perfluorocarboxylic acid) membrane stimulated using a train of square voltage pulses. In this case, as in our case, the bending angle was greater, and the bending speed was smaller using the tetrabutylammonium cation than the smaller sodium or lithium ions. This set of experiments is not strictly comparable to ours, since these workers used a gold-plated gel membrane that was suspended in water, not a salt solution. Their explanation of the data involved discussions of different water transport through the gel by the different ions and the suppression of water electrolysis by the tetra-*n*-butylammonium ion.

The dependence of t_{ss}, the time needed to reach the steady-state bending angle, on two concentrations of Cs_2SO_4 is shown in Figure 8 for both gels. This figure shows that the time needed to reach the steady-state bending angle appeared to be independent of the Cs_2SO_4 concentration in both gels. In fact, t_{ss} was independent of salt concentration in all salts in both gels studied in this work. However, t_{ss} varied with the nature of the surrounding salt for both our gels as shown in Figure 14, which shows this very distinctly. These times needed to reach the steady-state bending angle, as determined from the numerical bending angle data, are summarized in Table 4. For both gels, the time needed to reach the steady-state bending angle increased in the order of decreasing cation mobility, in the order Cs_2SO_4, Na_2SO_4, TMA, and TBA. In addition, in the same salt solution at the same concentration, in all salts, the time needed to reach the steady-state bending angle was

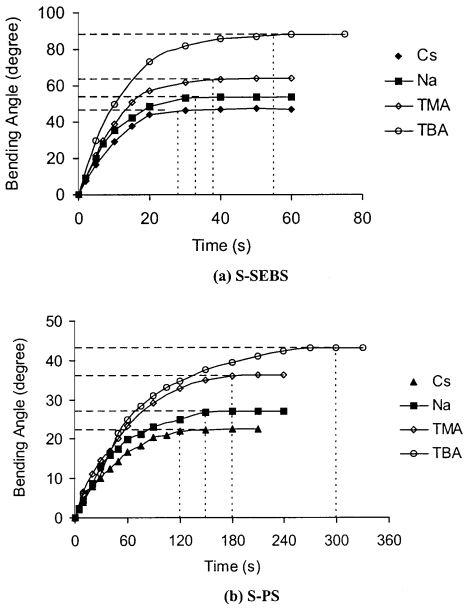

Figure 14. Bending angles vs time and t_{ss} of S-SEBS (a) and S-PS (b) in different salt solutions.

Table 4. Time Needed To Reach Steady-State Bending, t_{ss}, for the S-SEBS and the S-PS Gels in Different Salt Solutions[a]

salt	t_{ss} (s) (S-SEBS)	t_{ss} (s) (S-PS)
Cs_2SO_4	27 ± 5	108 ± 7
Na_2SO_4	33 ± 5	140 ± 15
TMA	38 ± 5	165 ± 15
TBA	55 ± 5	255 ± 15

[a] Error limits are mean deviations over all concentrations and also reflect the time intervals in which the data were analyzed numerically.

much shorter for the S-SEBS gel than for the S-PS gel. The ratio of t_{ss} of S-SEBS to that of S-PS increased slightly from Cs_2SO_4 to TBA in the four salts, from 4.0 to 4.6. In this connection, we may note that the ratio of the thickness of the wet S-PS gel to that of the wet S-SEBS gel was about 6.0, somewhat greater than the inverse of the t_{ss} ratio. These gels, therefore, did not have initial bending speeds proportional to the inverse 1.7 power of the thickness, unlike those of Homma et al.[15] But our two gels were rather different from each other, with very different types of cross-links and swelling ratios, so they should not be compared in the same way as those of Homma et al.[15]

Although our values of t_{ss}, the time needed to achieve the steady-state bending angle, were somewhat subjective, these times were very different in the different salts, and it thus seemed reasonable to look for a correlation with the drift velocity in the gels of the slower ions in the electric field. We decided to deal only with the cations for two reasons: (a) they are the major mobile ion species in each of our gels, and (b) in each of our four salts, the cations had a lower mobility than the anions (see Table 2). Assuming for simplicity that the time, t, needed for the average cation to cross the thickness of the gel is just the gel thickness divided by the drift speed of the ions, then

$$t = \frac{d}{s} = \frac{d}{\mu E} \tag{8}$$

where d is the thickness of the swollen gel slab, s is the drift velocity of the ion in the electric field, μ is the mobility of the ion, and E is the electric field strength. The curves in Figure 15 show how the t_{ss} should change in both gels as the cations are changed, assuming that the mobilities of the hydrated cations are the ones shown in Table 2 at all concentrations and do not change inside the gel. The data points are the experimentally determined times from Table 4. Considering all the assumptions needed to use eq 8, the agreement with experiment is gratifying, except that the predicted value of t_{ss} is quite a bit higher than the experimentally determined value at the lower values of drift velocity, especially in the thicker slab of S-PS. The greater drift speed of the anions may be important as a variable to decrease the time needed to reach the steady-state bending when the drift speed of the cations is low.

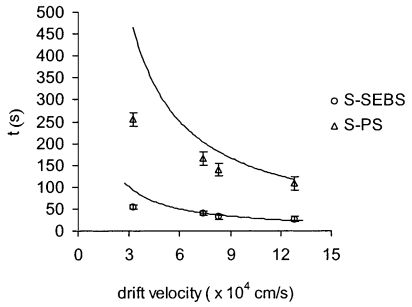

Figure 15. Time needed to reach the steady-state bending angle vs the drift velocity of the mobile cations. The curves were calculated from eq 8.

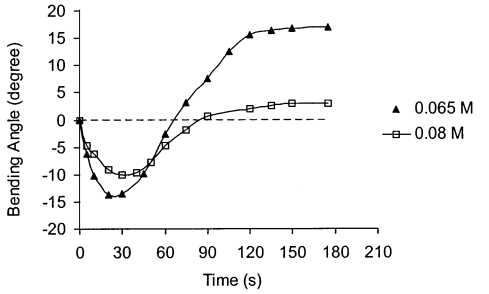

Figure 16. Bending angle vs time of the S-PS gel, preequilibrated in deionized water, in two TBA solutions. Positive bending angles are toward the cathode while negative bending angles are toward the anode. The dashed line indicates the original perpendicular position of the gel. The electric field of 1.6 V/cm was turned off at 180 s.

Bending of Gel Preequilibrated in Deionized Water. When an S-XL-PS gel was preequilibrated in deionized water and then placed quickly into an electrolyte solution without letting the gel equilibrate, the initial bending direction was not always toward the cathode. Three cases were observed: Case I consisted of bending toward the cathode after the field was applied, just like the gels preequilibrated in the appropriate salt solutions. Case I occurred when the surrounding electrolyte solutions were Cs_2SO_4 at all the concentrations studied, Na_2SO_4 and TMA (<0.08 M), and TBA (<0.065 M). Case II consisted of initial bending toward the anode, followed by bending toward the cathode. This behavior occurred in TBA solutions with concentration between 0.065 and 0.08 M (see Figure 16). Case III consisted of slow bending toward the anode at relatively high concentrations (0.09−0.1 M) of TBA, with an apparent approach to a steady-state bending angle after about 3 min. The field was turned off at the end of 3 min.

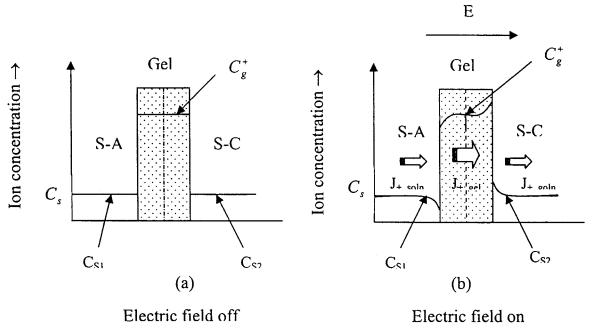

Figure 17. Ionic distributions in the gel and the surrounding electrolyte solution before (a) and after (b) the electric field is turned on. S-A and S-C indicate the solution, and C_{s1} and C_{s2} refer to the cation concentration at the anode and cathode side of the solution, respectively, and C_g^+ is the cation concentration in the gel. The arrows indicate the flux J_+ of the cations, and the thickness of the arrows indicates the magnitude of the flux, $J_{+,gel} > J_{+,soln}$.

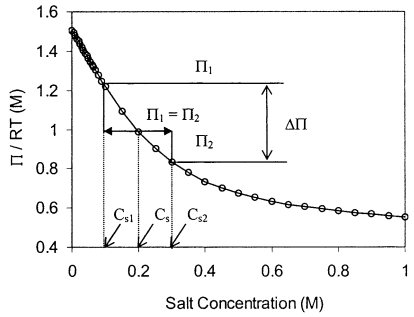

Figure 18. Osmotic pressure difference resulting from the local solution concentration changes at the two sides of the gel after the electric field is turned on. The original $\Pi_1 = \Pi_2$ and the steady-state values of Π_1 and Π_2 are arbitrary.

The initial bending toward the anode of the X-PS gels that were previously equilibrated in deionized water in the more concentrated TBA solutions can be explained using some of the same ideas that have been used previously to explain the bending of anionic gels toward the cathode. We essentially use the ideas of Doi et al.[13] If we simplify our anionically charged gel slab to a bilayer membrane with one layer facing the cathode and the other facing the anode, the bending phenomenon can be explained by differential swelling of the two gel layers induced by the transport of ions into and through the gel. Earlier, by comparing Figures 4 and 5, we showed that the equilibrium swelling of the membranes varied somewhat like the osmotic pressure difference across the boundary between the gel and the outside solution. In the present nonequilibrium case, we shall discuss the direction of gel bending in terms of the induced osmotic pressure difference between the two postulated gel layers; this should and does result in differential swelling. The two osmotic pressures will be called Π_1 and Π_2, where subscribe 1 and 2 refer to the gel layer facing the anode and the cathode, respectively, and $\Delta\Pi = \Pi_1 - \Pi_2$. When $\Pi_1 > \Pi_2$, $\Delta\Pi > 0$ and the gel bends toward the cathode; when $\Pi_1 < \Pi_2$, $\Delta\Pi < 0$ and the gel bends toward the anode. When $\Pi_1 = \Pi_2$, $\Delta\Pi = 0$ and no bending occurs; this is the situation in equilibrium swelling.

Before the electric field is applied, $\Delta\Pi = 0$, the gel is swollen to equilibrium and hangs straight down. When the electric field is applied, this original swelling equilibrium is broken by the movement of the mobile ions under the influence of the electric field. Such ionic motion causes local ionic concentration changes at the gel/solution boundaries of an anionic gel as shown in Figure 17. Figure 17 is based on numerical calculations made by Doi et al.[13] Those calculations involved considerations of the mobility of the mobile ions in the solution and gel and the Donnan equilibrium across each of the gel boundaries; the establishment of the Donnan equilibrium was assumed instantaneous with respect to the slower drift of the ions between the electrodes. Concentration-dependent diffusion of the ions was also considered. Figure 17 focuses on the distribution of the cations, the dominant mobile ions in our gels. The difference between the cation concentration across each gel/solution interface before the electric field is applied (Figure 17a) depends very much on the concentration of fixed negative charges in the swollen gel. The distribution of each ionic species is uniform across the gel layers and in the external solution. As soon as the electric field is turned on, the mobile cations, both inside the gel and in the surrounding solution, drift toward the cathode. Like Doi et al.,[13] we assume that the drift velocity of the ions in the gel is about the same as that in the surrounding solution. Consequently, the flux ($J = Cs$) of the cations in the gel is larger than that in the solution, as indicated by the width of the arrows in Figure 17b, $J_{+,gel} > J_{+,soln}$. The result of this is a depletion of cations on the solution side of the gel/solution boundary closer to the anode that, because of the Donnan equilibrium, also results in a decrease of cation concentration on the gel side of the same boundary. Another result of this cation flux is an increase of cation concentration on the solution side of the gel/solution boundary closer to the cathode that, again because of the Donnan equilibrium, also results in an increase of cation concentration on the gel side of the same boundary. The Donnan equilibrium, and thus the osmotic pressure difference across the two gel boundaries, is therefore based on two different salt concentrations on the solution sides of the membrane. Figure 18 shows what happens to these osmotic pressure differences in general terms and thus illustrates this electric field-induced $\Delta\Pi$. For the purpose of this discussion, the curve shown in Figure 18 is the same as the curve in Figure 5 that refers to the S-SEBS membrane in 1−2 salts, but extended to 1 M salt concentration; the curves in Figure 5 are shown only to 0.1 M salt concentration. We can see that the osmotic pressure difference across either interface is a decreasing function of the surrounding salt concentration. Figure 18 shows the equilibrium osmotic pressure difference, $\Pi_1 = \Pi_2$, $\Delta\Pi = 0$, before the electric field is turned on and also after the electric field has been on for a while. At that later time, Π_1 has increased while Π_2 has decreased. As a result, $\Delta\Pi > 0$ and the anode side gel layer swells more than the cathode side gel layer; the gel thus bends toward the cathode. A steady state is reached after a time, as can be seen experimentally and as was discussed earlier.

Similar considerations can be used to explain the bending behavior of some of our S-PS gels that had been preequilibrated in deionized water. When a slab of water-swollen S-PS gel is placed in any salt solution, the gel must shrink since the equilibrium osmotic pressure in the gel is much higher in water than in salt solution (extrapolation of Figure 5). If no electric field is applied, the shrinkage should be uniform at all directions. When the electric field is turned on before the new equilibrium is established, the shrinkage becomes nonuniform between the anode layer and

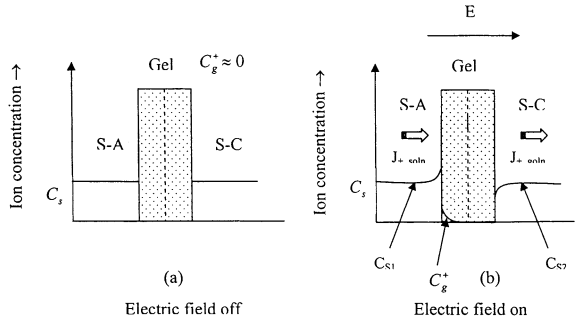

Figure 19. Distribution of the ions in a gel preequilibrated in deionized water and the surrounding salt solution before (a) and after (b) the electric field is turned on. The labels are the same as those for Figure 16.

cathode layer of the gel due to the electric field-induced motion of the ions. Figure 19a shows the distribution of the cations in the solution at the moment when the gel is placed in a fairly concentrated salt solution with low cation mobility, like a ≥0.065 M TBA solution. Soon after the electric field is applied, as shown in Figure 19b, the cation concentration on the solution side of the solution/gel interface at the anode side of the gel increases because the cation flux is much greater in the solution than in the gel. This happens even though some cations are leaving this part of the solution because of the Donnan effect, and some water is expelled from the gel due to shrinkage. On the cathode side of the gel, the cation concentration on the solution side of the solution/gel decreases since, again, the cation flux in the solution is much greater than in the gel. The movement of cations into the gel due to the Donnan effect and the movement of water out of the gel due to shrinkage exacerbate this effect. Therefore, in this case, the salt solution concentration at the anode side of solution near the gel surface (C_{s1}) increases while that at the cathode side of solution near the gel surface (C_{s2}) decreases. Because of the decreasing function of osmotic pressure as a function of external salt solution concentration (see Figure 18), $\Pi_1 < \Pi_2$, $\Delta\Pi < 0$, and the gel bends toward the anode at first. The S-SEBS gel did not bend toward the anode in any of the salt solutions. This probably due to its thinness; both the shrinkage and the movement of the ions through this membrane were much faster than in the S-PS.

Conclusions

1. Both the S-SEBS and the S-PS gels bent toward the cathode in a 1.7 V/cm dc field when preequilibrated in the corresponding salt solution. The bending angle increased linearly at the start and then more slowly toward a steady-state bending angle. The time needed to reach the steady-state bending angle was independent of the salt concentration but depended on the type of salt used. Both the steady-state bending angle and the initial speed of bending reached a maximum at the same intermediate salt concentration that changed little with type of salt or gel type. The steady-state bending angle decreased, while the initial bending speed increased as the mobility of the cation increased.

2. When the S-PS gel was preequilibrated in deionized water, it first bent toward the anode in a dc field in ≥0.065 M TBA solution but not in the other salt solutions. The S-SEBS gel did not bend toward the anode in any of the salt solutions.

Acknowledgment. Our thanks to Scott Lassell at the Ward Center, Cornell University, for help in using and interpreting the data from the Co-60 source and to Thomas Russell and Michael Pollard, University of Massachusetts, Amherst, for help with the SAXS experiments and data interpretation. Financial support from the Becton Dickinson Company, Franklin Lakes, NJ, the Office of Naval Research through Grant N00014-95-0136 and the National Science Foundation through Grant DMR-9521265 is gratefully acknowledged.

References and Notes

(1) Shiga, T. *Adv. Polym. Sci.* **1997**, *134*, 131.
(2) Tanaka, T.; Nishio, I.; Sund, S.; Ueno-Nishio, S. *Science* **1982**, *218*, 467.
(3) DeRossi, D. E.; Chiarell, P.; Buzzigoli, G.; Domenci, C. *Trans. Am. Soc. Artif. Intern. Organs* **1986**, *32*, 157.
(4) Osada, Y.; Hasebe, M. *Chem. Lett.* **1985**, 1285.
(5) Osada, Y.; Kishi, R.; Hasebe, M. *J. Polym. Sci., Part C: Polym. Lett.* **1987**, *25*, 481.
(6) Osada, Y.; Gong, J. P.; Sawahata, K. *J. Macromol. Sci., Chem.* **1991**, *A28* (11&12), 1189.
(7) Shiga, T.; Kurauchi, T. *J. Appl. Polym. Sci.* **1990**, *39*, 2305.
(8) Donnan, F. G. *Z. Elektrochem.* **1911**, *17*, 572.
(9) Kwon, I. C.; Bae, Y. H.; Kim, S. W. *J. Polym. Sci., Part B: Polym. Phys.* **1994**, *32*, 1085.
(10) Choi, O. S.; Yuk, S. H.; Lee, H. B.; Ihon, M. S. *J. Appl. Polym. Sci.* **1994**, *51*, 375.
(11) Ye, Y.; Rider, J. N.; Sekhar, A.; Wong, G.; Trout, K.; Grazyk, K.; Brown, W.; Gross, J.; Steward, M.; Kamler, M.; Wnek, G. *Polym. Prepr. (Am. Chem. Soc., Div. Polym. Chem.)* **1996**, *37*, 394.
(12) Ye, Y. Ph.D. Thesis, Department of Chemistry, Rensselaer Polytechnic Institute, Troy, NY, 1996.
(13) Doi, M.; Matsumoto, M.; Hirose, Y. *Macromolecules* **1992**, *25*, 5504.
(14) Makowski, H. S.; Lunderg, R. D.; Singhal, G. US Patent 3,-870,841, 1975.
(15) Homma, M.; Seida, Y.; Nakano, Y. *J. Appl. Polym. Sci.* **2000**, *75*, 111.
(16) Brown, D. S.; Wetton, R. E. In *Developments in Polymer Characterization;* Dawkins, J. V., Ed.; Applied Science Publishers: London, 1978; Vol. 1, Chapter 6.
(17) Spontak, R. J.; Williams, M. C.; Agard, D. A. *Polymer* **1988**, *189*, 2201.
(18) Liu, X.; Tong, Z.; Hu, O. *Macromolecules* **1995**, *28*, 3813.
(19) Oguro, K.; Fujiwara, N.; Asaka, K.; Onishi, K.; Sewa, S. Smart Materials and Structures. *Proc. SPIE* **1999**, *3669*, 64.
(20) *Lange's Handbook of Chemistry*, 15th ed.; Dean, J. A., Ed.; McGraw-Hill: New York, 1999.
(21) *CRC Handbook of Chemistry and Physics*, 80th ed.; Lide, D. R., Ed.; CRC Press: Boca Raton, FL, 1999.

MA021326Q